

Magnetism and superconductivity in $M_c\text{Ta}_2\text{S}_2\text{C}$ ($M = \text{Fe}, \text{Co}, \text{Ni}, \text{and Cu}$)

Masatsugu Suzuki* and Itsuko S. Suzuki†

Department of Physics, State University of New York at Binghamton, Binghamton, New York 13902-6000

Jürgen Walter‡

*Department of Materials Science and Processing, Graduate School of Engineering,
Osaka University, 2-1, Yamada-oka, Suita, 565-0879, JAPAN*

(Dated: March 23, 2022)

Magnetic properties of $M_c\text{Ta}_2\text{S}_2\text{C}$ ($M = \text{Fe}, \text{Co}, \text{Ni}, \text{Cu}$) have been studied using SQUID DC and AC magnetic susceptibility. In these systems magnetic M^{2+} ions are intercalated into van der Waals gaps between adjacent S layers of host superconductor $\text{Ta}_2\text{S}_2\text{C}$. $\text{Fe}_{0.33}\text{Ta}_2\text{S}_2\text{C}$ is a quasi 2D XY-like antiferromagnet on the triangular lattice. It undergoes an antiferromagnetic phase transition at T_N ($= 117$ K). The irreversible effect of magnetization occurs below T_N , reflecting the frustrated nature of the system. The AF phase coexists with two superconducting phases with the transition temperatures $T_{cu} = 8.8$ K and $T_{cl} = 4.6$ K. $\text{Co}_{0.33}\text{Ta}_2\text{S}_2\text{C}$ is a quasi 2D Ising-like antiferromagnet on the triangular lattice. The antiferromagnetic phase below $T_N = 18.6$ K coexists with a superconducting phase below $T_{cu} = 9.1$ K. Both $\text{Ni}_{0.25}\text{Ta}_2\text{S}_2\text{C}$ and $\text{Cu}_{0.60}\text{Ta}_2\text{S}_2\text{C}$ are superconductors with T_{cu} ($= 8.7$ K for Ni and 6.4 K for Cu) and T_{cl} ($= 4.6$ K common to $M_c\text{Ta}_2\text{S}_2\text{C}$). Very small effective magnetic moments suggest that Ni^{2+} and Cu^{2+} spins are partially delocalized.

PACS numbers: 74.70.Dd, 75.50.Ee, 75.40.Cx, 74.25.Ha

I. INTRODUCTION

$X_2\text{S}_2\text{C}$ ($X = \text{Ta}$ and Nb) belongs to the class of layered chalcogenides, where a sandwiched structure of $X\text{-C-X-S-S-X}$ is periodically stacked along the c axis. The structure of $X_2\text{S}_2\text{C}$ can be viewed as a structural sum of $X\text{-C}$ layer and $X\text{S}_2$ layered structure. There are very weak bonds between adjacent S layers, which is called van der Waals (vdw) gap. The structural and physical properties have been studied by several research groups.^{1,2,3,4,5,6,7,8,9} These compounds show superconductivity at low temperatures. Various kinds of transition metals M ($= \text{Ti}, \text{V}, \text{Cr}, \text{Mn}, \text{Fe}, \text{Co}, \text{Ni}, \text{Cu}$) can be intercalated into the host system $X_2\text{S}_2\text{C}$, forming intercalation compounds denoted by $M_cX_2\text{S}_2\text{C}$, where c is the concentration of M atoms. The basic structure of the host crystal remains unchanged. The structural and magnetic properties of $M_c\text{Ta}_2\text{S}_2\text{C}$ and $M_c\text{Nb}_2\text{S}_2\text{C}$ have been reported by Boller and Sobczak¹⁰ and Boller and Hiebl,⁶ respectively. The system $M_cX_2\text{S}_2\text{C}$ with $M = \text{V}, \text{Cr}, \text{Mn}, \text{Fe}, \text{Co}, \text{and Ni}$ has a c -axis stacking sequence denoted by a $3\text{R-}M_cX_2\text{S}_2\text{C}$ with a periodicity of three $X\text{-C-X-S-M-S-X}$ sandwiched structures, where M is located in octahedral sites in the vdw gaps between adjacent S layers. In contrast, $\text{Cu}_cX_2\text{S}_2\text{C}$ has a c -axis stacking sequence denoted by $1\text{T-Cu}_cX_2\text{S}_2\text{C}$, where Cu atoms are tetrahedrally coordinated by S atoms inside the S layers. The intercalate M layer forms a regular triangular lattice (the lattice constant a) in $3\text{R-}M_c\text{Ta}_2\text{S}_2\text{C}$, which is either commensurate or incommensurate with the in-plane structure of the host lattice. Since the in-plane structure of the host also forms a triangular lattice (the lattice constant $a_0 = 3.30\text{\AA}$), the ratio of a/a_0 is related to the concentration c as $a/a_0 = (1/c)^{1/2}$. The

nearest neighbor distance a is equal to $2a_0$ ($= 6.6\text{\AA}$) for $c = 1/4$ forming a (2×2) commensurate structure, and it is equal to $\sqrt{3}a_0$ ($= 5.72\text{\AA}$) for $c = 1/3$ forming a $(\sqrt{3} \times \sqrt{3})$ commensurate structure.

In our previous paper⁸ we have reported the superconductivity of the pristine $\text{Ta}_2\text{S}_2\text{C}$. It undergoes successive superconducting transitions of a hierarchical nature at $T_{cl} = 3.61 \pm 0.01$ K and $T_{cu} = 8.9 \pm 0.1$ K. The intermediate phase between T_{cu} and T_{cl} is an intra-grain superconductive state occurring in the TaC-type structure in $\text{Ta}_2\text{S}_2\text{C}$. The low temperature phase below T_{cl} is an inter-grain superconductive state. In this paper we have undertaken an extensive study on the magnetic and superconducting properties of $M_c\text{Ta}_2\text{S}_2\text{C}$ ($M = \text{Fe}, \text{Co}, \text{Ni}, \text{Cu}$) from SQUID (superconducting quantum interference device) DC and AC magnetic susceptibility. $M_c\text{Ta}_2\text{S}_2\text{C}$ exhibits a variety of superconducting and antiferromagnetic (AF) phase transitions, depending on the kind of M . The magnetic properties of $M_c\text{Ta}_2\text{S}_2\text{C}$ ($M = \text{Fe}, \text{Co}$) are mainly determined by magnetic behaviors of magnetic M^{2+} ions in a crystal field such that the anion octahedra surrounding the M^{2+} ions are trigonally elongated along the c -axis. In Sec. II we present a simple review on the spin Hamiltonian of Fe^{2+} and Co^{2+} under the trigonal crystal field. We show that both $\text{Fe}_{0.33}\text{Ta}_2\text{S}_2\text{C}$ and $\text{Co}_{0.33}\text{Ta}_2\text{S}_2\text{C}$ undergo an AF phase transition at T_N ($T_N = 117$ K for Fe and 18.6 K for Co), reflecting the frustrated nature of the systems. Like the pristine $\text{Ta}_2\text{S}_2\text{C}$, $M_c\text{Ta}_2\text{S}_2\text{C}$ ($M = \text{Fe}, \text{Co}, \text{Ni}, \text{Cu}$) also undergoes superconducting phase transitions at T_{cu} and T_{cl} , where T_{cu} is dependent on the kind of M^{2+} ions, while T_{cl} ($= 4.6$ K) is common to all our systems.

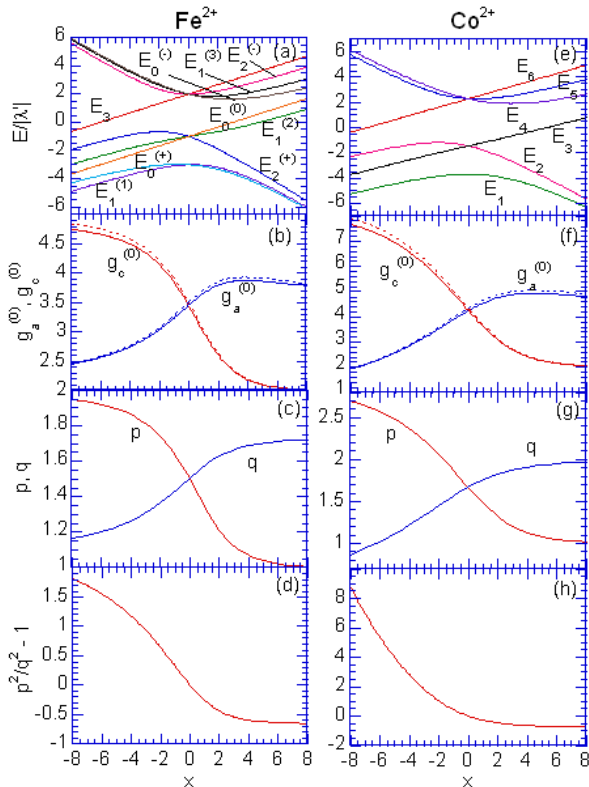


FIG. 1: (Color online) Derivation from Fe^{2+} spin Hamiltonian: (a) the energy levels, (b) g -factors $g_c^{(0)}$ and $g_a^{(0)}$ with k ($= 0.9$ (solid line) and 1 (dotted line)), (c) spin anisotropy parameters p and q , and (d) $p^2/q^2 - 1$, as a function of x ($= \delta_0/\lambda'$). $x = -1.27$ for $\text{Fe}_{0.33}\text{Ta}_2\text{S}_2\text{C}$. Derivation from Co^{2+} spin Hamiltonian: (e) the energy levels, (f) g -factors $g_c^{(0)}$ and $g_a^{(0)}$ with k ($= 0.9$ (solid line) and 1 (dotted line)), (g) spin anisotropy parameters p and q , and (h) $p^2/q^2 - 1$, as a function of x ($= \delta_0/\lambda'$). $x = 1.68$ for $\text{Co}_{0.33}\text{Ta}_2\text{S}_2\text{C}$.

II. BACKGROUND

A. Spin Hamiltonian of Fe^{2+} in the trigonal crystal field

The free-ion $3d^6$ 5D state of the Fe^{2+} is split by the cubic crystal field into the orbital doublet (E) and orbital triplet (T_2), the latter being the lowest one.^{11,12} We consider the splitting of the orbital triplet by the perturbing Hamiltonian given by

$$H_0 = -\lambda' \mathbf{l} \cdot \mathbf{S} - \delta_0 (l_z^2 - 2/3), \quad (1)$$

where $\lambda' = k\lambda$ ($k \approx 1$ but less than unity) and S is the spin angular momentum of the magnitude 2. A fictitious angular momentum \mathbf{l} of the magnitude 1 is antiparallel to the real orbital angular momentum \mathbf{L} ($= -k\mathbf{l}$). Figure 1(a) shows the splitting of the ground orbital triplet by the spin-orbit coupling λ' (< 0) and the trigonal field δ_0 , where each energy level E normalized by $|\lambda'|$ is plotted as a function of x ($= \delta_0/\lambda'$).

All the energy states except for $E_1^{(1)}$ and $E_0^{(+)}$ might be neglected, since these lowest levels lie 100 cm^{-1} below the others. Thus we may use a fictitious spin $s = 1$ for the lowest three states for the singlet ($E = E_0^{(+)}$) and for the doublet ($E = E_1^{(1)}$). The g -factors can be evaluated as $g_c = g_c^{(0)} + \Delta g$ and $g_a = g_a^{(0)} + \Delta g$, where Δg is due to the effect of spin-orbit coupling in admixing the upper orbital levels into the ground three orbitals. Figure 1(b) shows the g -factors $g_c^{(0)}$ and $g_a^{(0)}$ as a function of x with k as a parameter ($k = 0.9$ and 1): $g_c^{(0)} > g_a^{(0)}$ for $x < 0$ and $g_c^{(0)} < g_a^{(0)}$ for $x > 0$. Note that $x = -1.27$ for FeCl_2 . If we take the z axis parallel to the c axis, and x, y axes perpendicular to it, we have $S_x = qs_x$, $S_y = qs_y$, and $S_z = ps_z$. In Fig. 1(c) we show the parameters p and q as a function of x : $p > q$ for $x < 0$ and $p < q$ for $x > 0$. The resultant spin Hamiltonian for Fe^{2+} is given by

$$H = -2J \sum_{\langle i,j \rangle} \mathbf{s}_i \cdot \mathbf{s}_j - D \sum_i (s_{iz}^2 - 2/3) - 2J_A \sum_{\langle i,j \rangle} s_{iz} s_{jz}, \quad (2)$$

where $\langle i, j \rangle$ denotes the nearest neighbor pairs, $J = q^2 K$ and K is the isotropic exchange energy with the form of $-2KS_i \cdot S_j$ between the real spins S_i and S_j , $D \approx \delta_0/10$ (> 0) is the single ion anisotropy, and J_A ($= ((p^2 - q^2)/q^2)J$) (see Fig. 1(d)) is the anisotropic exchange interaction. The spin anisotropy parameter D_{eff} is defined as $D_{eff} = D(s - 1/2) + 2z s J_A$.

B. Spin Hamiltonian of Co^{2+} in the trigonal crystal field

In a cubic crystal field the free-ion $3d^7$ 4F state is split into two orbital triplets and one orbital singlet with a triplet the lowest.^{11,13,14} We consider the splitting of the ground state orbital triplet 4T_1 into six Kramers doublets. The perturbing Hamiltonian consists of the spin-orbit coupling and trigonal distortion of the crystal field,

$$H_0 = -(3/2)\lambda' \mathbf{l} \cdot \mathbf{S} - \delta_0 (l_z^2 - 2/3), \quad (3)$$

where S is the spin angular momentum of the magnitude $3/2$ and a fictitious angular momentum \mathbf{l} of the magnitude 1 is antiparallel to the real orbital angular momentum L ($= -3k\mathbf{l}/2$). Figure 1(e) shows the energy level E of the six Kramers doublets normalized by $|\lambda'|$, as a function of x ($= \delta_0/\lambda'$).

For all values of x , $E_{\pm 1}$ is the lowest energy. Since there are only two states in this lowest Kramers doublet, the true spin S ($= 3/2$) can be replaced by a fictitious spin s ($= 1/2$) within the ground state. The correction Δg is due to the effect of spin-orbit coupling in admixing the upper orbital levels into the ground orbital triplet. Figure 1(f) shows the values of $g_a^{(0)}$ and $g_c^{(0)}$ as a function of x with k as a parameter ($k = 0.9$ and 1.0). Figure 1(g) shows the parameters p and q as a function of x : $p > q$ for $x < 0$ and $p < q$ for $x > 0$. The spin Hamiltonian of

Co^{2+} may be written by Eq.(2) without the second term. The ratio J_A/J ($= (p^2 - q^2)/q^2$) (see Fig. 1(h)) provides a measure for the spin symmetry of the system.

III. EXPERIMENTAL PROCEDURE

Powdered samples of $M_c\text{Ta}_2\text{S}_2\text{C}$ ($M = \text{Fe}, \text{Co}, \text{Ni}, \text{Cu}$) were prepared by Wally and Ueki,⁹ where $c = 0.33$ for $M = \text{Fe}, \text{Co}$, $c = 0.25$ for Ni , and 0.60 for Cu . The detail of the synthesis and structural characterization by x-ray diffraction was described by Wally and Ueki.⁹ The measurements of DC and AC magnetic susceptibility were carried out using a SQUID magnetometer (Quantum Design MPMS XL-5). Before setting up samples at 298 K, a remnant magnetic field was reduced to less than 3 mOe using an ultra-low field capability option. For convenience, hereafter this remnant field is noted as the state $H = 0$. The ZFC and FC susceptibility (χ_{ZFC} and χ_{FC}) were measured after a ZFC protocol, which consists of (i) cooling of the system from 298 to 1.9 K at $H = 0$ and (ii) applying H at 1.9 K. The susceptibility χ_{ZFC} was measured with increasing T from 1.9 to 200 K. After annealing the system at 250 K (typically) for 1200 sec, χ_{FC} was measured with decreasing T from 200 to 1.9 K. The detail of the measurements of DC and AC magnetic susceptibility is described in Sec. IV.

IV. RESULT

A. Paramagnetic susceptibility

Figure 2 shows the T dependence of χ_{FC} at $H = 10$ kOe of $M_c\text{Ta}_2\text{S}_2\text{C}$ ($M = \text{Fe}, \text{Co}, \text{Ni}$) and at $H = 500$ Oe for $M = \text{Cu}$. The susceptibility obeys a Curie-Weiss law,

$$\chi_g = \chi_g^0 + C_g/(T - \Theta), \quad (4)$$

where Θ (K) is the Curie-Weiss temperature, C_g (emu K/g) is the Curie-Weiss constant, and χ_g^0 (emu/g) is the T -independent susceptibility. The gram susceptibility χ_g of $M_c\text{Ta}_2\text{S}_2\text{C}$ is related to the molar susceptibility χ_M by $\chi_M = \zeta_M \chi_g$, where the molar mass is defined by $\zeta_M = (M_0c + 438.039)$ (g/mole) and M_0 is the molar mass of M ion. The molar Curie constant C_M (emu K/M mole) [$= \zeta_M C_g = (N_A \mu_B^2 P_{eff}^2)/3k_B$] is related to an effective magnetic moment P_{eff} by $C_M = P_{eff}^2/8$. The least-squares fits of the data of χ_{FC} vs T for $150 \leq T \leq 298$ K to Eq.(4) yield the parameters (Θ , C_g , and χ_g^0) listed in Table I.

We find that Θ is negative for $M_c\text{Ta}_2\text{S}_2\text{C}$ with $M = \text{Fe}^{2+}, \text{Co}^{2+}, \text{Ni}^{2+}$, and Cu^{2+} ions, suggesting the AF nature of the intraplanar exchange interaction between M^{2+} spins. $M_c\text{Ta}_2\text{S}_2\text{C}$ magnetically behaves like a quasi two-dimensional (2D) AF. Structurally the interplanar distance ($\approx 8.6\text{\AA}$) between M ions in the adjacent M layers is longer than the intraplanar distance

($\sqrt{3}a_0 = 5.72\text{\AA}$) for $c = 1/3$ between M^{2+} ions in the same M layer. The existence of S-Ta-C-Ta-S sandwiched layered structures greatly reduces the interplanar exchange interaction between M^{2+} ions in the adjacent vdw gaps. Then the intraplanar exchange interaction J can be estimated using the relation $\Theta = 2zJs(s+1)/3k_B$, where z ($= 6$) is the number of the nearest neighbor M atoms. The values of J and spin s for $M_c\text{Ta}_2\text{S}_2\text{C}$ are listed in Table II, where $s = S = 1$ for Ni^{2+} and $1/2$ for Cu^{2+} .

The T -independent gram-susceptibility (χ_g^0) of $M_c\text{Ta}_2\text{S}_2\text{C}$ is positive. The paramagnetic nature of $M_c\text{Ta}_2\text{S}_2\text{C}$ arises from magnetic M^{2+} ions. This is in contrast to the diamagnetic nature of the pristine $\text{Ta}_2\text{S}_2\text{C}$. Note that χ_{FC} of $\text{Ta}_2\text{S}_2\text{C}$ takes a negative constant (diamagnetic susceptibility) above 150 K: $\chi_g^0(\text{Ta}_2\text{S}_2\text{C}) = (-1.44 \pm 0.01) \times 10^{-7}$ emu/g at 298 K. The T -independent molar susceptibility (χ_M^0) of $M_c\text{Ta}_2\text{S}_2\text{C}$, as listed in Table II, is related to χ_g^0 as $\chi_M^0 = \zeta_M \chi_g^0$. The value of χ_M^0 for $M = \text{Co}$ is much larger than that for $M = \text{Fe}, \text{Ni}$, and Cu . The diamagnetic contribution from $\text{Ta}_2\text{S}_2\text{C}$ is subtracted from χ_g^0 for $\text{Co}_{0.33}\text{Ta}_2\text{S}_2\text{C}$. The effective molar susceptibility (χ_M^0) _{c} of $\text{Co}_{0.33}\text{Ta}_2\text{S}_2\text{C}$ can be calculated as $(7.61 \pm 0.68) \times 10^{-4}$ emu/Co mole) using the relation

$$(\chi_M^0)_c = [m\chi_g^0(\text{Co}_x\text{Ta}_2\text{S}_2\text{C}) - m_0\chi_g^0(\text{Ta}_2\text{S}_2\text{C})]/c,$$

with $c = 0.33$, where m and m_0 is the molar mass of $\text{Co}_c\text{Ta}_2\text{S}_2\text{C}$ and $\text{Ta}_2\text{S}_2\text{C}$, respectively. Such a large value of (χ_M^0) _{c} may be partly due to the Van Vleck susceptibility of Co^{2+} spin arising from the narrow energy difference between the ground state with E_1 and five Kramers doublets with $E_2 - E_6$.¹³ For $x = 1.68$ and $k = 0.9$ for Co^{2+} spin, the Van Vleck susceptibility can be calculated as $\chi_V^z = 4.19N_A\mu_B^2/(|\lambda|)$ and $\chi_V^x = 7.29N_A\mu_B^2/(|\lambda|)$, where N_A is the Avogadro number. The Van Vleck susceptibility for the powdered system [$= (2\chi_V^x + \chi_V^z)/3$] is estimated as 9.1×10^{-3} emu/Co mole. Thus our value of (χ_M^0) _{c} cannot be well explained only from this model.

B. χ_{ZFC} and χ_{FC} at $H = 1$ Oe

We have measured the T dependence of χ_{ZFC} and χ_{FC} at $H = 1$ Oe for $M_c\text{Ta}_2\text{S}_2\text{C}$. Figure 3(a) shows the T dependence of χ_{ZFC} , χ_{FC} , and δ ($= \chi_{FC} - \chi_{ZFC}$) for $\text{Fe}_{0.33}\text{Ta}_2\text{S}_2\text{C}$. Both χ_{ZFC} and χ_{FC} have a kink at 4.5 K and a peak at 8.7 K. The sign of χ_{ZFC} at $H = 1$ Oe is negative below 92 K. Note that for $H \geq 10$ Oe, the sign of χ_{ZFC} is positive at any T (see Fig. 4). The susceptibility χ_{FC} , whose sign is positive at any T and H , exhibits a drastic increases below 117 K with decreasing T and almost saturates below 60 K.

The deviation δ drastically increases with decreasing T below 117 K, suggesting the frustrated nature of the system (the 2D antiferromagnet on the triangular lattice). The negative sign of χ_{ZFC} below 92 K at $H = 1$ Oe

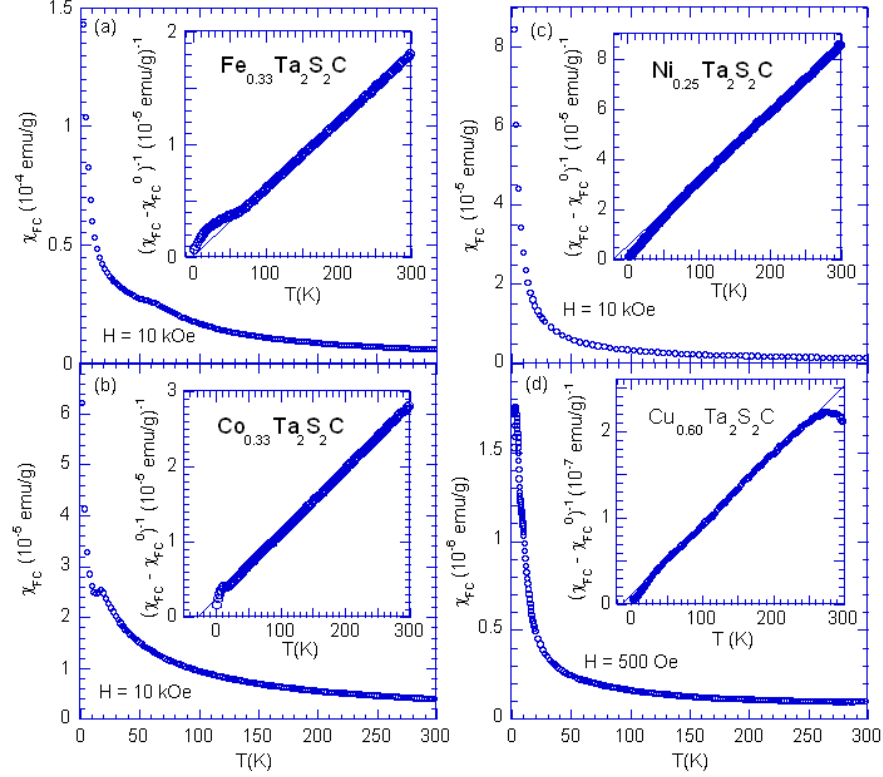


FIG. 2: (Color online) T dependence of (a) χ_{FC} at $H = 10$ kOe for $\text{Fe}_{0.33}\text{Ta}_2\text{S}_2\text{C}$, (b) χ_{FC} at $H = 10$ kOe for $\text{Co}_{0.33}\text{Ta}_2\text{S}_2\text{C}$, (c) χ_{FC} at $H = 10$ kOe for $\text{Ni}_{0.25}\text{Ta}_2\text{S}_2\text{C}$, and (d) χ_{FC} at $H = 500$ Oe for $\text{Cu}_{0.60}\text{Ta}_2\text{S}_2\text{C}$. The inset shows the T dependence of the reciprocal susceptibility $(\chi_{FC} - \chi_{FC}^0)^{-1}$. The solid lines denote the least squares fitting curves to the Curie-Weiss law given by Eq.(4). The fitting parameters are listed in Table I.

TABLE I: Magnetic susceptibility data of $M_c\text{Ta}_2\text{S}_2\text{C}$ ($M = \text{Fe}, \text{Co}, \text{Ni}, \text{and Cu}$). The least-squares fitting parameters determined from the data of $\chi_g (= \chi_{FC})$ vs T for $150 \leq T \leq 298$ K. The definition of the parameters is given in the text.

M_c	$P_{eff}(\mu_B)$	$\Theta(\text{K})$	$\chi_g^0 (10^{-7} \text{ emu/g})$	$\chi_M^0 (10^{-4} \text{ emu/M mole})$
$\text{Fe}_{0.33}$	4.47 ± 0.03	-9.8 ± 1.6	0.91 ± 0.61	1.26 ± 0.84
$\text{Co}_{0.33}$	3.57 ± 0.04	-26.3 ± 2.4	4.11 ± 0.48	5.70 ± 0.67
$\text{Ni}_{0.25}$	2.32 ± 0.03	-19.7 ± 3.9	0.14 ± 0.28	0.26 ± 0.52
$\text{Cu}_{0.60}$	0.28 ± 0.01	-13.7 ± 0.8	0.51 ± 0.06	0.40 ± 0.01

TABLE II: Parameters of spin Hamiltonian for $M_c\text{Ta}_2\text{S}_2\text{C}$. s is a fictitious spin and S is a spin predicted from the Hund rule. J is the intraplanar exchange interaction.

M_c	s	S	g	J (K)
$\text{Fe}_{0.33}$	1	2	3.16 ± 0.02	-1.22 ± 0.20
$\text{Co}_{0.33}$	1/2	3/2	4.12 ± 0.05	-8.75 ± 0.78
$\text{Ni}_{0.25}$	-	1	1.64 ± 0.02	-2.46 ± 0.49
$\text{Cu}_{0.60}$	-	1/2	0.324 ± 0.003	-4.57 ± 0.27

may be related to the diamagnetic susceptibility of the pristine $\text{Ta}_2\text{S}_2\text{C}$ as a host,⁸ which is a feature common to systems having 1T-TaS₂ type structure.¹⁵ We note

that the value of χ_{ZFC} at $H = 1$ Oe and $T = 1.9$ K is -2.5×10^{-4} emu/g for $\text{Fe}_{0.33}\text{Ta}_2\text{S}_2\text{C}$, which is in contrast to that ($\chi_{ZFC} = -1.7 \times 10^{-3}$ emu/g) for $\text{Ta}_2\text{S}_2\text{C}$ as a type II superconductor.

Figure 3(b) shows the T dependence of χ_{ZFC} , χ_{FC} , and δ at $H = 1$ Oe for $\text{Co}_{0.33}\text{Ta}_2\text{S}_2\text{C}$. The susceptibility χ_{ZFC} has peaks at 10.0 and 18.6 K, while χ_{FC} has peaks at 9.8 K and 18.6 K. The peaks at 10 K and 18.6 K are related to the superconductivity ($T_{cu} = 9.1$ K) and the AF spin ordering ($T_N = 18.6$ K). Both χ_{ZFC} and χ_{FC} are negative at low T , while the deviation δ , which is positive at any T , decreases drastically with increasing T and reduces to zero at higher T . This system undergoes a superconducting transition at T_{cu} at which δ tends to reduce to zero.

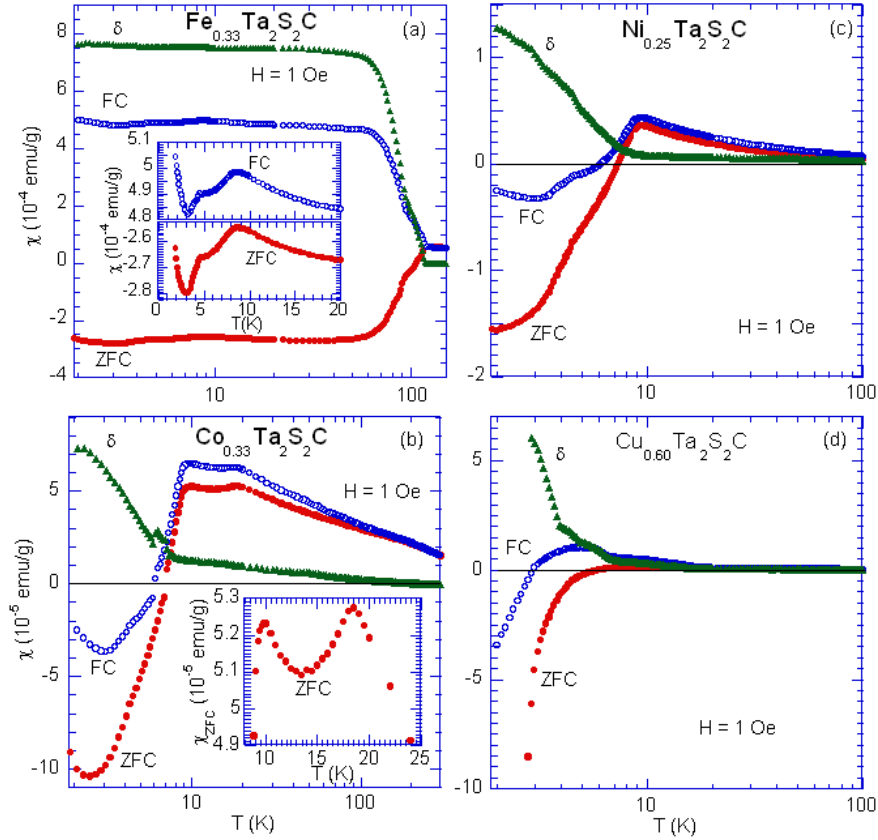


FIG. 3: (Color online) T dependence of χ_{ZFC} , χ_{FC} , and δ ($= \chi_{FC} - \chi_{ZFC}$) for (a) $\text{Fe}_{0.33}\text{Ta}_2\text{S}_2\text{C}$, (b) $\text{Co}_{0.33}\text{Ta}_2\text{S}_2\text{C}$, (c) $\text{Ni}_{0.25}\text{Ta}_2\text{S}_2\text{C}$, and (d) $\text{Cu}_{0.60}\text{Ta}_2\text{S}_2\text{C}$. $H = 1$ Oe. The units of (c) and (d) are the same as those of (a) and (b), respectively.

Figure 3(c) shows the T dependence of χ_{ZFC} , χ_{FC} , and δ at $H = 1$ Oe for $\text{Ni}_{0.25}\text{Ta}_2\text{S}_2\text{C}$. The susceptibility χ_{FC} at $H = 1$ Oe shows a local minimum at 3.0 K and a broad peak at 9.40 K, while χ_{ZFC} shows a peak at 9.40 K. The deviation δ exhibits a step-like change at 9.85 K. This system undergoes a superconducting transition at $T_{cu} = 8.69 \pm 0.04$ K, at which the data of $d\delta/dT$ vs T has a local minimum (see Sec. IV E).

Figure 3(d) shows the T dependence of χ_{ZFC} , χ_{FC} , and δ at $H = 1$ Oe for $\text{Cu}_{0.60}\text{Ta}_2\text{S}_2\text{C}$. The susceptibility χ_{FC} shows a broad peak at 4.9 K, while χ_{ZFC} shows a broad peak around 8 - 9 K. The deviation δ exhibits three step-like changes around 2.9, 3.9 and 6.5 K. This system undergoes a superconducting transition at $T_{cu} = 6.4$ K, at which the data of $d\delta/dT$ vs T has a local minimum.

C. $\text{Fe}_{0.33}\text{Ta}_2\text{S}_2\text{C}$

In Figs. 4(a) and (b) we show the T dependence of χ_{ZFC} and χ_{FC} at $H (= 1, 2, 5, \text{ and } 10 \text{ Oe})$ for $\text{Fe}_{0.33}\text{Ta}_2\text{S}_2\text{C}$, respectively. In Fig. 5 we show the T dependence of χ_{ZFC} , χ_{FC} , and δ at low H for $\text{Fe}_{0.33}\text{Ta}_2\text{S}_2\text{C}$. The susceptibility χ_{ZFC} at $H = 1$ and 2 Oe is negative below 106 K and 93 K, respectively. In

contrast, χ_{ZFC} above 10 Oe and χ_{FC} at any H are positive at any T . The susceptibility χ_{ZFC} at $H = 1$ Oe shows two peaks at T_{cu} ($= 8.8$ K) and T_N ($= 117$ K), and two cusps at T_{cl} ($= 4.6$ K) and T'_N (≈ 94 K). The susceptibility χ_{FC} (typically at 20 Oe) starts to increase with decreasing T around T_N . It shows a peak at T_{cu} , and a cusp at T_{cl} . The deviation δ at $H = 20$ Oe, for example, undergoes step-like increases around T_N and T_{cu} , indicating that the irreversible effect of magnetization occurs. At $H = 1200$ Oe there is no appreciable difference between χ_{ZFC} and χ_{FC} at any T . Note that δ is almost equal to zero above T_N . The deviation δ (typically at $H = 5$ and 20 Oe) shows step-like changes at T_N , T'_N , and T_{cu} , with decreasing T .

Figure 6 shows the T dependence of χ_{ZFC} (emu/Fe mole) at $H = 5, 20, \text{ and } 300$ Oe, where $\chi_{ZFC}(\text{emu/Fe mole}) = \zeta_{Fe}\chi_{ZFC}(\text{emu/g})$ with $\zeta_{Fe} = 1383.23$ g/Fe mole. The susceptibility χ_{ZFC} at $H = 20$ Oe exhibits peaks around T_{cl} , T_{cu} , T'_N , and T_N , while χ_{ZFC} at $H = 300$ Oe shows a broad peak around T_{cu} . The peak values of χ_{ZFC} are 0.036 emu/Fe mole at T_{cu} and 0.03 emu/Fe mole at T_N , respectively. Note that the T dependence of the DC susceptibility χ of $\text{Fe}_c\text{Nb}_2\text{S}_2\text{C}$ ($c = 0.4, 0.5, \text{ and } 0.6$) between 80 and 550 K has been reported by Boller and Hiebl.⁶ The susceptibility χ exhibits

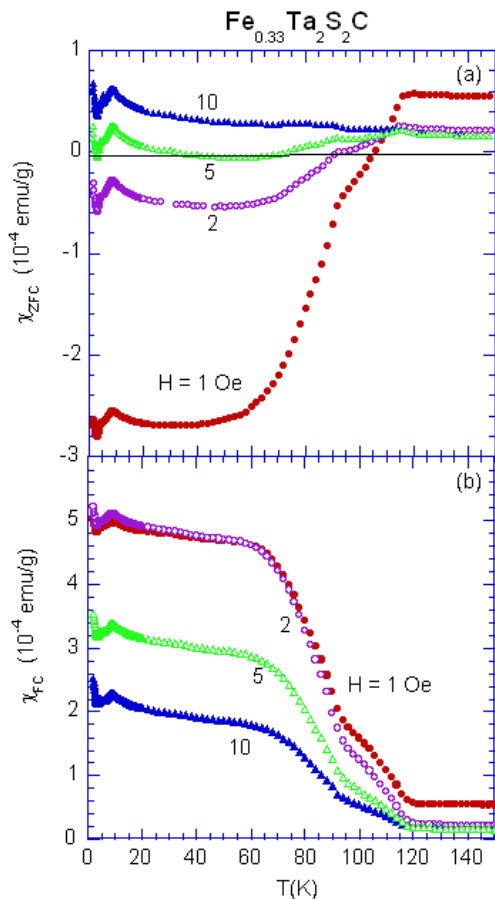


FIG. 4: (Color online) T dependence of (a) χ_{ZFC} and (b) χ_{FC} at H ($= 1, 2, 5,$ and 10 Oe) for $\text{Fe}_{0.33}\text{Ta}_2\text{S}_2\text{C}$.

a cusp-like behavior at a peak temperature T_p , which decreases with decreasing Fe concentration c : $T_p = 346$ K at $c = 0.6$ and $T_p = 180$ K at $c = 0.4$. An extrapolation of the possible linear relation of T_p vs c may lead to $T_p = 137$ K at $c = 0.33$, suggesting that a possible peak temperature T_p in $\text{Fe}_{0.33}\text{Nb}_2\text{S}_2\text{C}$ may correspond to T_N in $\text{Fe}_{0.33}\text{Ta}_2\text{S}_2\text{C}$. The magnetic neutron powder diffraction of $\text{Fe}_{0.5}\text{Nb}_2\text{S}_2\text{C}$ shows no evidence for the possible long range spin order below $T_p = 305$ K (Boller).¹⁶

In Fig. 7(a) we show the H dependence of M at $T = 1.9$ K for $\text{Fe}_{0.33}\text{Ta}_2\text{S}_2\text{C}$. The magnetization M was measured by changing H in sequence from 0 to 1 kOe, from 1 kOe to -1 kOe, and from -1 kOe to 1 kOe, after the sample was cooled from 298 K to 1.9 K in the absence of H . The magnetization M slightly shows a magnetic hysteresis. The inset of Fig. 7(a) shows the H dependence of M_{ZFC} at $T = 1.9$ K, where the measurement was carried out after the ZFC cooling from 298 to 1.9 K in the absence of H . The value of M_{ZFC} is negative at $H = 0$ and increases with increasing H . The sign of M_{ZFC} changes around $H = 2.6$ Oe from negative to positive. It increases with further increasing H .

Figure 7(b) shows the H dependence of the M_{FC} (in

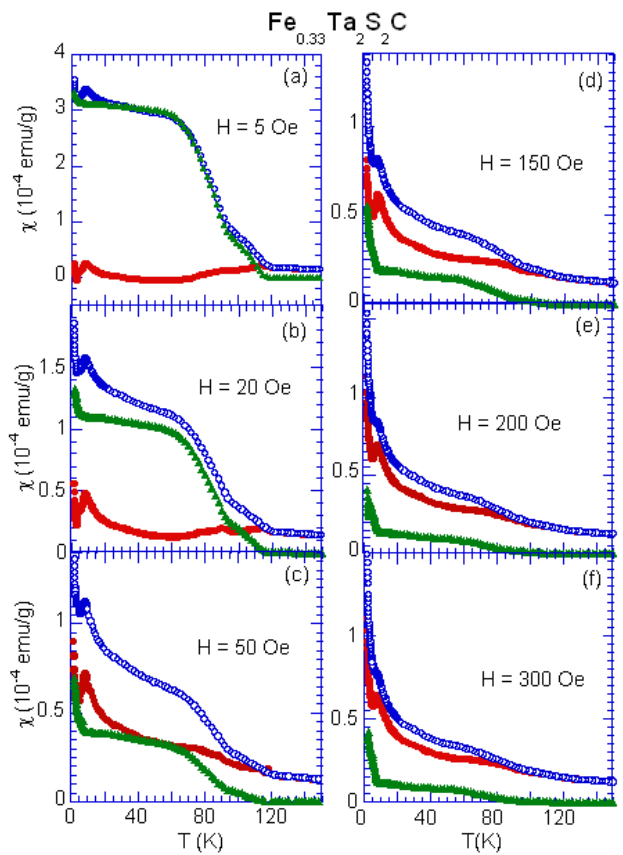


FIG. 5: (Color online) (a)-(f) T dependence of χ_{ZFC} , χ_{FC} , and δ at various H for $\text{Fe}_{0.33}\text{Ta}_2\text{S}_2\text{C}$. The units of (d)-(f) are the same as those of (a)-(c).

the units of emu/Fe mole) divided by $N_A\mu_B$ ($= 5584.94$ emu/Fe mole) at various T for $\text{Fe}_{0.33}\text{Ta}_2\text{S}_2\text{C}$. No appreciable hysteresis effect is observed: the M - H curve with increasing H is almost the same as that with decreasing H . The saturation magnetization M_s is equal to $N_A\mu_B g s$ ($= 17648.4$ emu/Fe mole), when g ($= 3.16 \pm 0.02$) and the fictitious spin ($s = 1$) for Fe^{2+} are assumed. The magnetization M_{FC} reaches 4.56×10^3 emu/Fe mole at $H = 45$ kOe and $T = 1.9$ K, corresponding to $M/M_s = 0.26$, which is close to $1/3$ corresponding to the metamagnetic plateau in the M - H curve observed in quasi 2D XY -like AF on the triangular lattice C_6Eu (Eu^{2+} with $S = 7/2$).^{17,18,19}

Figures 8(a) and (b) show the T dependence of the dispersion χ' and the absorption χ'' in the absence of H where the amplitude of the AC field is $h = 1$ Oe and the AC frequency f is between 0.05 Hz and 100 Hz. After the sample was cooled from 298 to 1.9 K at $H = 0$, the AC susceptibility was measured at fixed T as a function of f during the process of increasing T from 1.9 to 13 K. The dispersion χ' shows a cusp at T_{cl} and peak around T_{cu} , while χ'' decreases with increasing T and reduces to zero above T_{cu} . No frequency dependence of χ' and χ'' is observed. Figures 8(c) and (d) show the T dependence

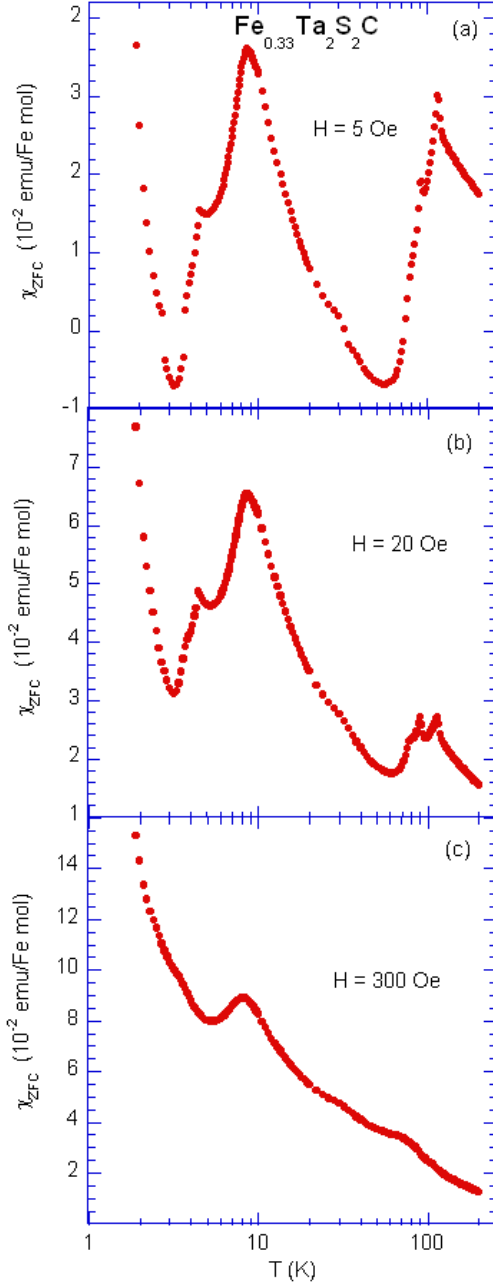


FIG. 6: (Color online) (a)-(c) T dependence of χ_{ZFC} (emu/Fe mole) at H (= 5, 20, and 300 Oe) for $\text{Fe}_{0.33}\text{Ta}_2\text{S}_2\text{C}$.

of χ' and χ'' in the presence of H , where $f = 0.1$ Hz and $h = 1$ Oe. The shift of the peak at T_{cu} to the low- T side with increasing H . The absorption χ'' is slightly dependent on H below $T_{cl}(H)$.

In Fig. 9 we show the H - T diagram for $\text{Fe}_{0.33}\text{Ta}_2\text{S}_2\text{C}$, where the temperatures of peaks or cusps of χ_{ZFC} vs T and χ' vs T at various H are plotted as a function of H . There are four lines denoted by $H_{c2}^{(l)}(T)$, $H_{c2}^{(u)}(T)$, $H'_N(T)$, and $H_N(T)$ which correspond to $T_{cl}(H)$, $T_{cu}(H)$, $T'_N(H)$, and $T_N(H)$, respectively. The two lower temper-

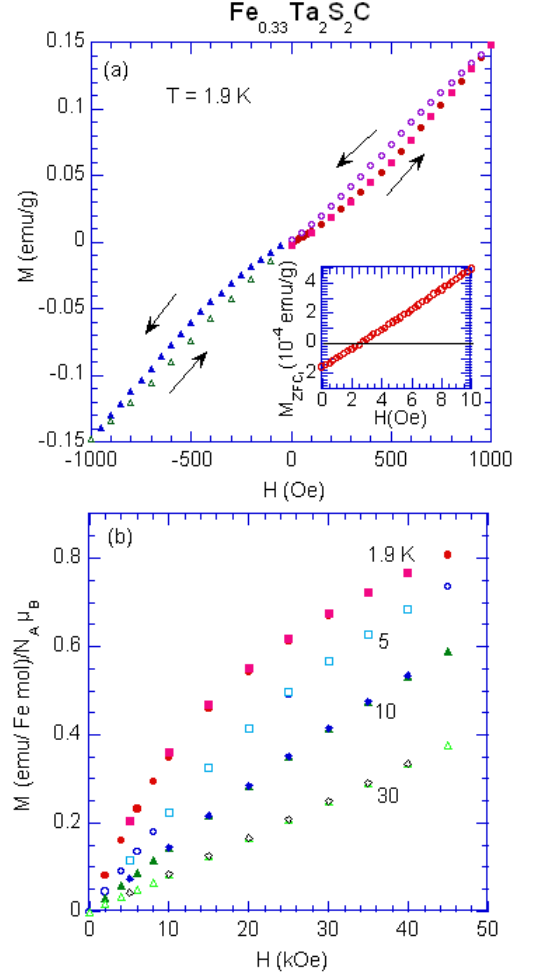


FIG. 7: (Color online) (a) H dependence of M at $T = 1.9$ K for $\text{Fe}_{0.33}\text{Ta}_2\text{S}_2\text{C}$. The measurement of M was made by changing H in sequence from 0 to 1 kOe (M coincides with M_{ZFC}), from 1 kOe to -1 kOe, and from -1 kOe to 1 kOe, after the sample was cooled from 298 K to 1.9 K in the absence of H . The inset shows the H dependence of M_{ZFC} at $T = 1.9$ K. (b) H dependence of M_{FC} at various T for $\text{Fe}_{0.33}\text{Ta}_2\text{S}_2\text{C}$.

atures (T_{cu} and T_{cl}) are related to the onset of superconductivity in the sample in the pristine $\text{Ta}_2\text{S}_2\text{C}$ sample. The phase transition at T_N (= 117 K), where the ZFC and FC curves split, is most likely associated with an AF magnetic ordering of the spin system. The possible transition at T'_N (= 94 K) may be assigned to some change of this magnetic structure. The magnetic ordering occurs within the intercalated magnetic layers and does not destroy the superconducting transition that occurs at lower temperature.

The ratio η ($= T_N/|\Theta|$) provides a measure for the degree of the deviation from a molecular field theory. It is known that the ratio η is smaller than 1 for conventional spin systems and tends to decrease with the change of the dimension d from 3 to 2, typically $T_N/|\Theta| = 0.49$ for FeCl_2 ,^{20,21} 0.65 for CoCl_2 ,^{21,22} and 0.77 for NiCl_2 .^{21,23} It

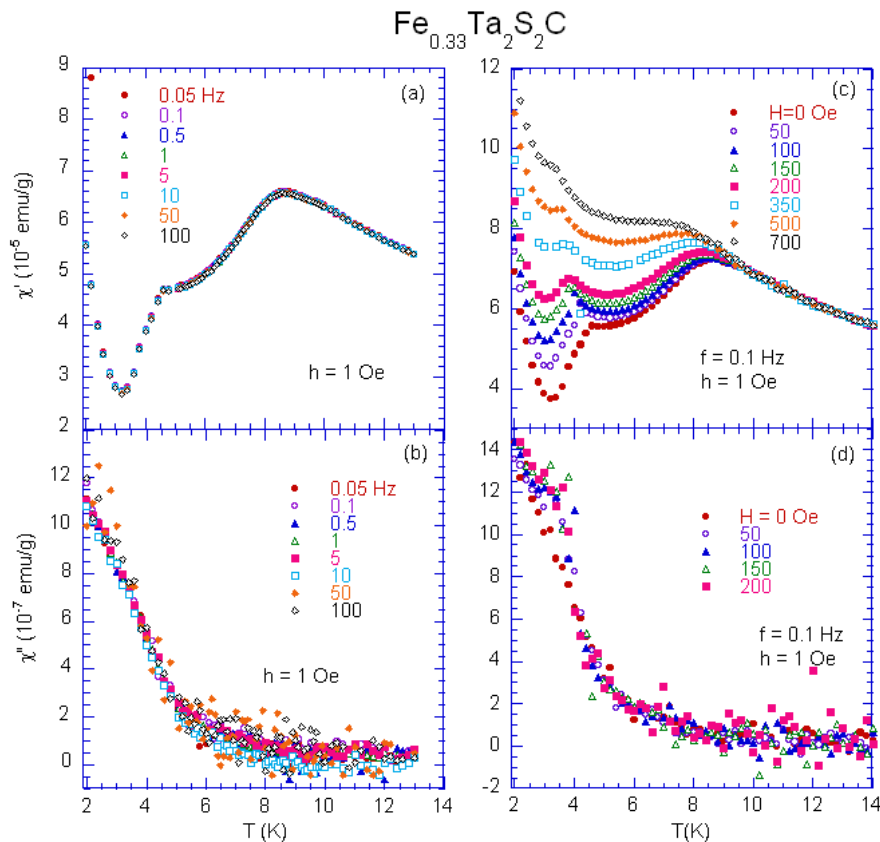


FIG. 8: (Color online) T dependence of (a) χ' and (b) χ'' at f ($= 0.05 - 100$ Hz) for $\text{Fe}_{0.33}\text{Ta}_2\text{S}_2\text{C}$. $h = 1$ Oe. T dependence of (c) χ' and (d) χ'' at various H for $\text{Fe}_{0.33}\text{Ta}_2\text{S}_2\text{C}$. $f = 0.1$ Hz. $h = 1$ Oe. The units of (c) and (d) are the same as those of (a) and (b), respectively. Note that the background part of χ' and χ'' at $f = 0.1$ Hz and $h = 1$ Oe in (a) and (b) is different from those in (c) and (d). These two measurements were carried out independently. The method of the measurements is different: (a) and (b) for the f scan at each fixed T and (c) and (d) for the T scan at $f = 0.1$ Hz as T was increased at each H (after each T scan, H was increased at 14 K and then T was decreased to 1.9 K in the presence of H).

is unexpected that AF magnetic phase transition occurs at such a high temperature as 117 K, when the derived Θ is only -9.8 K. However, a Curie-Weiss temperature Θ derived from a limited temperature window does not tell all about the interactions in the system. The Fe^{2+} ions from an triangular lattice with the side having the in-plane distance 5.72\AA for $\text{Fe}_{0.33}\text{Ta}_2\text{S}_2\text{C}$. Since the c -axis stacking sequence is Ta-C-Ta-S-Fe-S-Ta, the interaction between Fe^{2+} spins is considered to be a superexchange interaction between nearest neighbor Fe^{2+} spins through a superexchange path Fe-S-Fe. This exchange interaction is roughly estimated as $|J| = 15$ K if T_N is equal to $|\Theta|$ ($= 8|J|$). At present we have no explanation for the origin of such a large $|J|$.

D. $\text{Co}_{0.33}\text{Ta}_2\text{S}_2\text{C}$

Figure 10(a) shows the hysteresis loop of the magnetization M at $T = 1.9$ K. After the sample was quenched from 298 to 1.9 K at $H = 0$, the measurement was car-

ried out with varying H from 0 to 2 kOe at T , from $H = 2$ to -2 kOe, and from $H = -2$ to 2 kOe. The M - H curve at 1.9 K shows a large hysteresis and a remnant magnetization. Structural imperfections or defect in the sample may play a role of flux pinning, resulting in an inhomogeneous type-II superconductor. Figure 10(b) shows typical data of M_{ZFC} vs H at various T . Before each measurement, the sample was kept at 20 K at $H = 0$ for 1200 sec and then it was quenched from 20 K to T (< 4 K). The magnetization M_{ZFC} at T was measured with increasing H ($0 \leq H \leq 700$ Oe). The magnetization M_{ZFC} exhibits a single local minimum at a characteristic field for $T < T_{cu}$, shifting to the low- H side with increasing T . The local minimum field at 1.9 K (≈ 350 Oe) for $\text{Co}_{0.33}\text{Ta}_2\text{S}_2\text{C}$ is much higher than that at 1.9 K for the pristine $\text{Ta}_2\text{S}_2\text{C}$ ($= 60$ Oe). The lower critical field $H_{c1}(T)$ is defined not as the first minimum point of the M_{ZFC} vs H , but as the first deviation point from the linear portion due to the penetration of magnetic flux into the sample: $H_{c1}(T = 1.9 \text{ K}) = 65 \pm 5$ Oe. Using a conventional relation²⁴ $H_{c1}(T) = H_{c1}(0)[1 - (T/T_{cu})^2]$

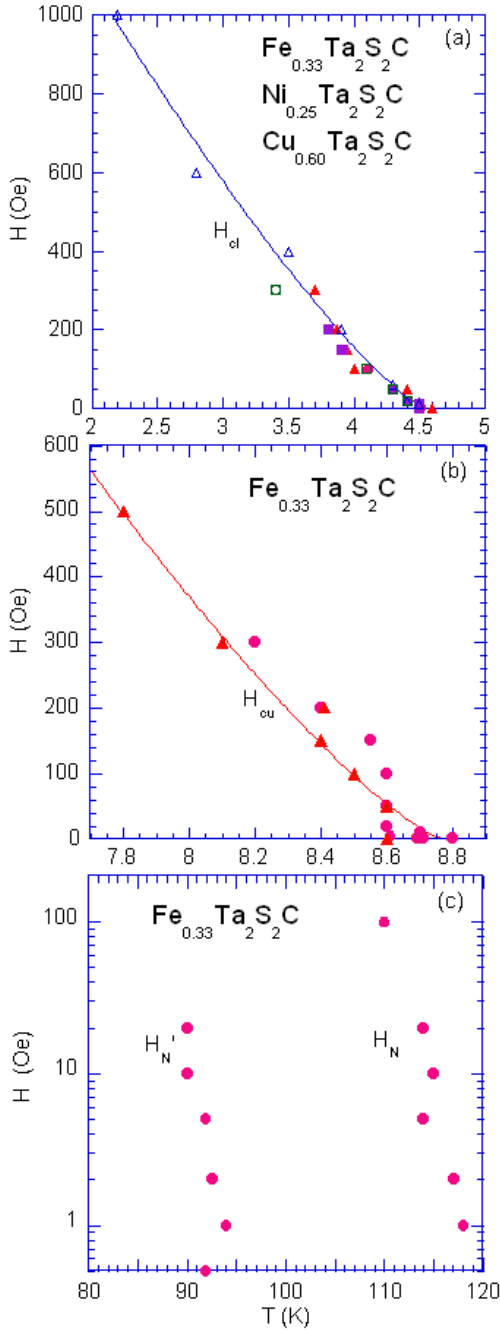


FIG. 9: (Color online) H - T diagram of $M_c\text{Ta}_2\text{S}_2\text{C}$. (a) The line $H_{c1}(T)$ for $\text{Fe}_{0.33}\text{Ta}_2\text{S}_2\text{C}$ [peak temperatures of χ_{ZFC} vs T (\bullet), χ_{FC} vs T (\blacksquare), and χ' vs T (\blacktriangle) as a function of H], $\text{Ni}_{0.25}\text{Ta}_2\text{S}_2\text{C}$ [peak temperatures of χ_{ZFC} vs T (\circ) and χ_{FC} vs T (\square) as a function of H], and $\text{Cu}_{0.60}\text{Ta}_2\text{S}_2\text{C}$ [peak temperatures of χ_{FC} vs T (\triangle) as a function of H]. (b) The line $H_{cu}(T)$ for $\text{Fe}_{0.33}\text{Ta}_2\text{S}_2\text{C}$: peak temperatures of χ_{ZFC} vs T (\bullet) and χ' vs T (\blacktriangle) as a function of H . (c) The lines $H'_N(T)$ and $H_N(T)$ for $\text{Fe}_{0.33}\text{Ta}_2\text{S}_2\text{C}$: peak temperatures of χ_{ZFC} vs T (\bullet) as a function of H . The solid lines of (a) and (b) denote least-squares fitting curves of the data to the power law form Eq.(5).

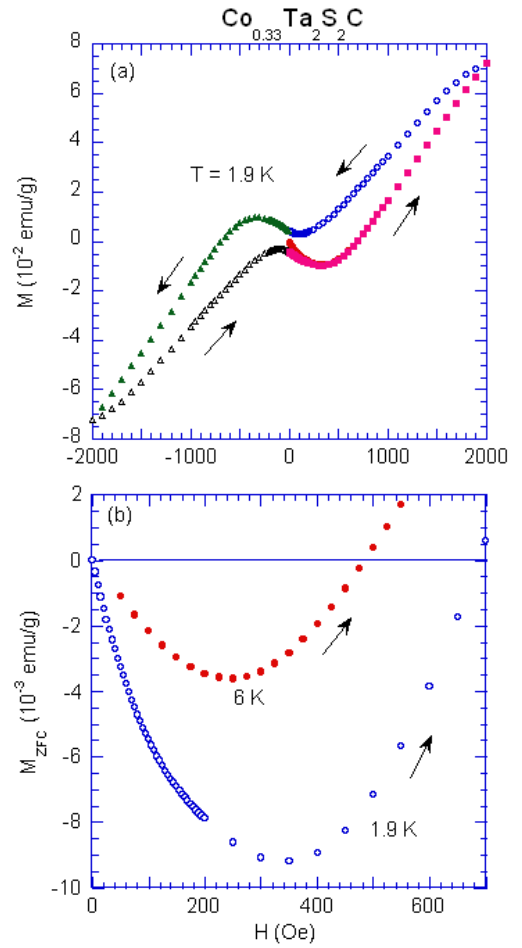


FIG. 10: (Color online) (a) Magnetization curve (M vs H) at $T = 1.9$ K for $\text{Co}_{0.33}\text{Ta}_2\text{S}_2\text{C}$. (b) Detail of M_{ZFC} vs H at $T = 1.9$ and 6.0 K.

with $T_{cu} = 9.14 \pm 0.03$ K, $H_{c1}(0)$ can be estimated as 68 ± 5 Oe. Note that no demagnetization factor is taken into account in deriving $H_{c1}(T)$.

Figures 11(a) and (b) show the T dependence of χ' and χ'' for $\text{Co}_{0.33}\text{Ta}_2\text{S}_2\text{C}$, where $f = 1$ Hz and $h = 0.5$ Oe. The T dependence of χ' and χ'' is strongly dependent on H . Below the critical temperature $T_{cu}(H)$, the sign of χ' and χ'' is negative and positive, respectively, suggesting the existence of the Meissner effect.

Figures 11(c) and (d) show the T dependence of χ_{ZFC} and χ_{FC} for $\text{Co}_{0.33}\text{Ta}_2\text{S}_2\text{C}$ at various H . In Fig. 12, we show the T dependence of δ for $\text{Co}_{0.33}\text{Ta}_2\text{S}_2\text{C}$. In Fig. 13(a) we show the plot of $T_{cu}(H)$ as a function of H , where $T_{cu}(H)$ is defined as a temperature at which χ' at H coincides with that at $H = 7$ kOe. We find that $T_{cu}(H)$ is almost equal to a temperature at which δ exhibits a kink just after a drastic decrease in δ with increasing T . An upward curvature in $H_{c2}^{(u)}$ vs T indicates that $H_{c2}^{(u)}(T)$ can be described by

$$H_{c2}^{(u)}(T) = H_{c2}^{(u)}(T=0)(1 - T/T_{cu})^{\alpha(u)}, \quad (5)$$

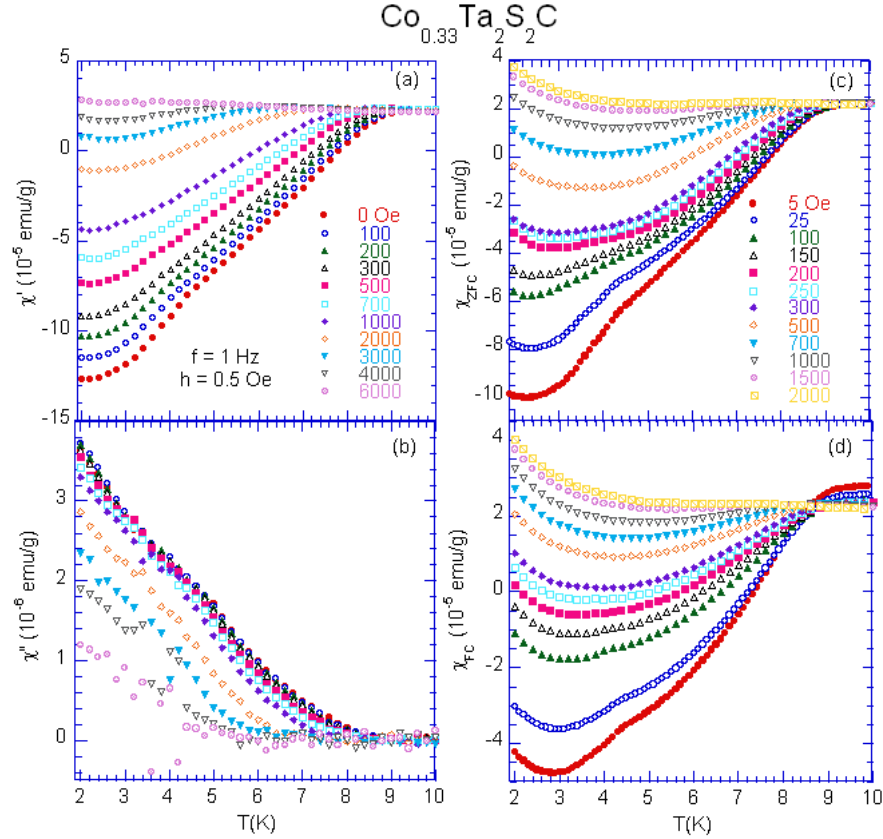


FIG. 11: (Color online) T dependence of (a) χ' and (b) χ'' at various H for $\text{Co}_{0.33}\text{Ta}_2\text{S}_2\text{C}$. $f = 1$ Hz. $h = 0.5$ Oe. T dependence of (c) χ_{ZFC} and (d) χ_{FC} at various H for $\text{Co}_{0.33}\text{Ta}_2\text{S}_2\text{C}$.

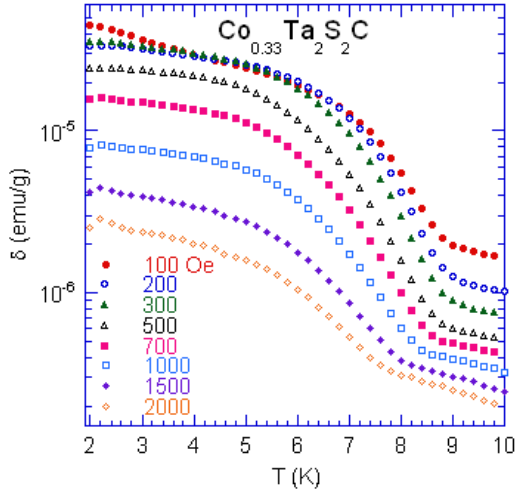


FIG. 12: (Color online) T dependence of δ for $\text{Co}_{0.33}\text{Ta}_2\text{S}_2\text{C}$.

with an exponent $\alpha(u)$ being larger than 1. The least-squares fit of the data of $H_{c2}^{(u)}$ vs T to Eq.(5) yields the parameters $H_{c2}^{(u)}(0) = 17.1 \pm 1.0$ kOe, $T_{cu} = 9.1 \pm 0.1$ K, and $\alpha(u) = 1.35 \pm 0.06$. The values of T_{cu} and $H_{c2}^{(u)}(0)$

for $\text{Co}_{0.33}\text{Ta}_2\text{S}_2\text{C}$ are slightly larger than those for the pristine $\text{Ta}_2\text{S}_2\text{C}$, respectively; $T_{cu} = 8.9 \pm 0.1$ K and $H_{c2}^{(u)}(0) = 14.0 \pm 0.5$ kOe for $\text{Ta}_2\text{S}_2\text{C}$.⁸ In $\text{Co}_{0.33}\text{Ta}_2\text{S}_2\text{C}$, the superconductivity occurring in the Ta-C layer may compete with the possible charge density wave (CDW) effect occurring in the 1T-TaS₂ layered structure.¹⁵ The slight enhancement of T_{cu} in $\text{Co}_{0.33}\text{Ta}_2\text{S}_2\text{C}$ may be related to a suppression of the possible CDW.

The coherence length ξ and the magnetic penetration depth λ are related to $H_{c1}(0)$ and $H_{c2}(0)$ through relations $H_{c1}(0) = (\Phi_0/4\pi\lambda^2) \ln(\lambda/\xi)$ and $H_{c2}(0) = \Phi_0/(2\pi\xi^2)$,²⁴ where $\Phi_0 (= 2.0678 \times 10^{-7}$ Gauss cm²) is the fluxoid. When the values of $H_{c1}(0) (= 68$ Oe) and $H_{c2}^{(u)}(0) (= 17.1$ kOe) are used, the values of the Ginzburg-Landau parameter $\kappa (= \lambda/\xi)$, λ and ξ can be estimated as $\kappa = 19.3 \pm 0.3$, $\xi = 80 \pm 10 \text{ \AA}$ and $\lambda = 1560 \pm 100 \text{ \AA}$ for $\text{Co}_{0.33}\text{Ta}_2\text{S}_2\text{C}$.

E. $\text{Ni}_{0.25}\text{Ta}_2\text{S}_2\text{C}$ and $\text{Cu}_{0.60}\text{Ta}_2\text{S}_2\text{C}$

In Figs. 14-17 we show the T dependence of χ_{ZFC} , χ_{FC} , and δ for $\text{Ni}_{0.25}\text{Ta}_2\text{S}_2\text{C}$ and $\text{Cu}_{0.60}\text{Ta}_2\text{S}_2\text{C}$. These results are similar to those for $\text{Co}_{0.33}\text{Ta}_2\text{S}_2\text{C}$. The negative sign of χ_{ZFC} and χ_{FC} indicates that the super-

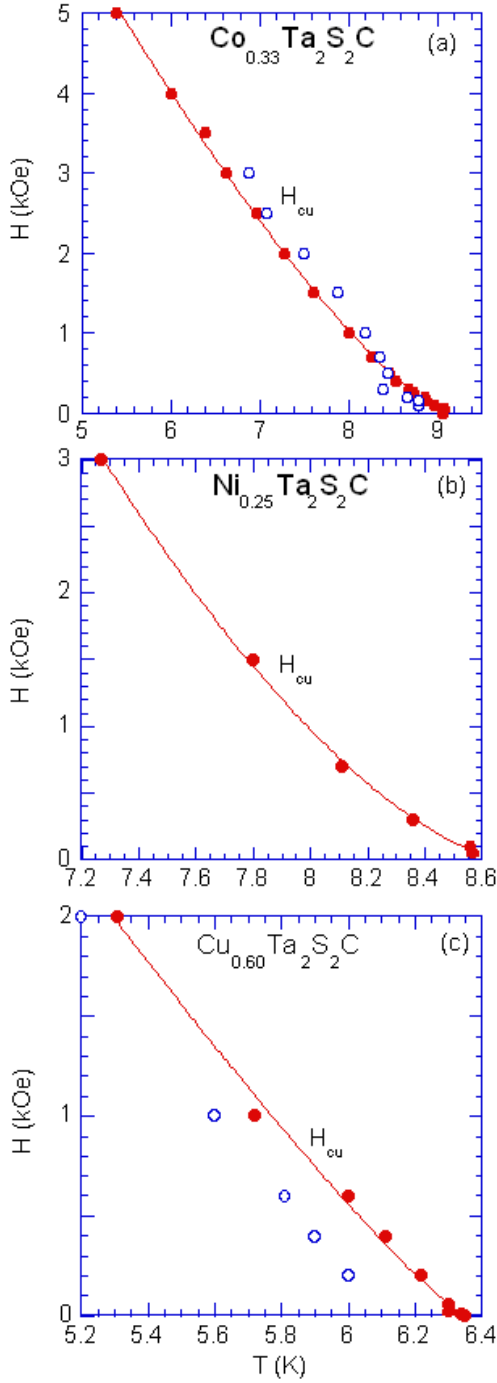


FIG. 13: (Color online) (a) H - T diagram for $\text{Co}_{0.33}\text{Ta}_2\text{S}_2\text{C}$: $H_{cu}(T)$ determined from the data of χ' vs T (closed circles) and δ vs T (open circles) with H . (b) H - T phase diagram for $\text{Ni}_{0.25}\text{Ta}_2\text{S}_2\text{C}$: $H_{cu}(T)$ determined from the data of δ vs T with H . (c) H - T phase diagram for $\text{Cu}_{0.60}\text{Ta}_2\text{S}_2\text{C}$: $H_{cu}(T)$ determined from the data of $d\delta/dT$ vs T (closed circle) and $d\chi_{ZFC}/dT$ vs T (open circle) with H . The solid lines denote least-squares fitting curves to the power law form Eq.(5).

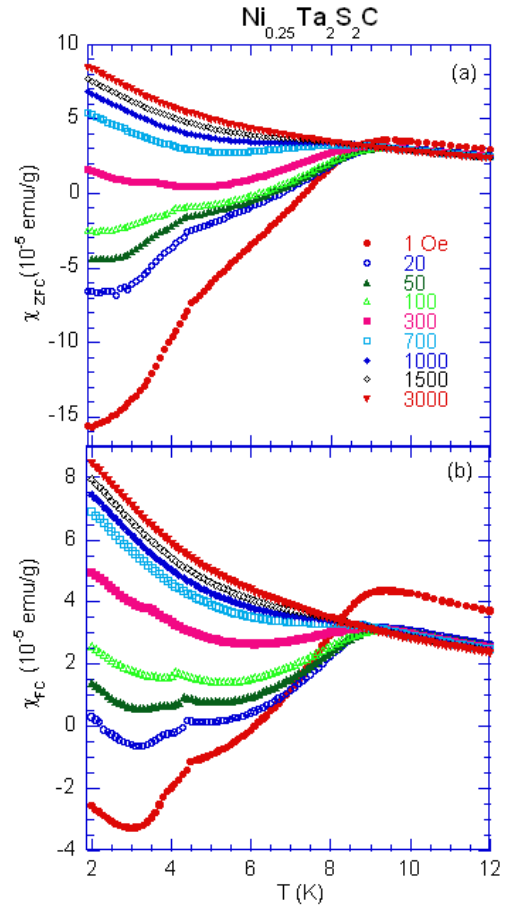


FIG. 14: (Color online) T dependence of (a) χ_{ZFC} and (b) χ_{FC} for $\text{Ni}_{0.25}\text{Ta}_2\text{S}_2\text{C}$ at various H .

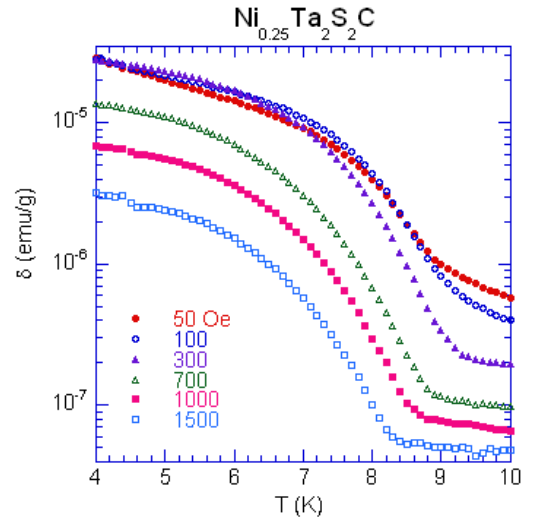


FIG. 15: (Color online) T dependence of δ for $\text{Ni}_{0.25}\text{Ta}_2\text{S}_2\text{C}$ at various H . Note that it is difficult to derive the value of T at which δ tends to zero for each H , from this figure since the value of δ is plotted in a logarithmic scale, as a function of T .

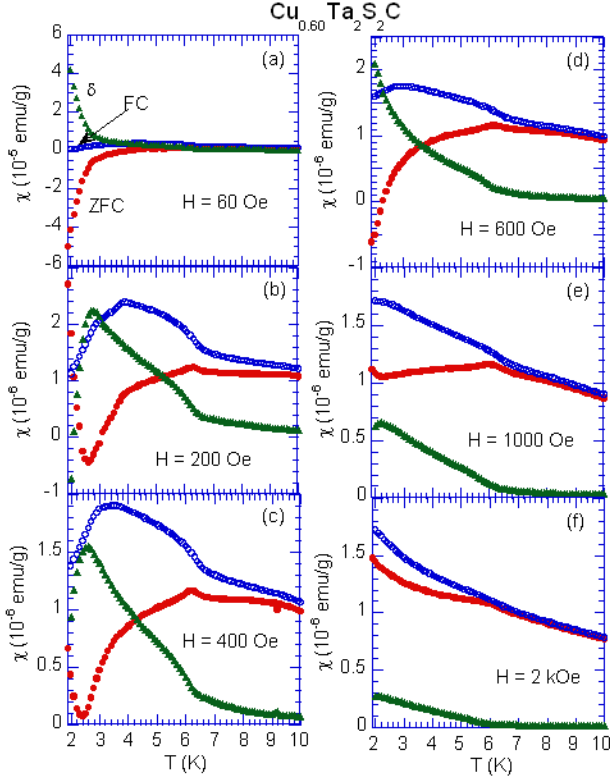


FIG. 16: (Color online) (a) - (f) T dependence of χ_{ZFC} , χ_{FC} , and δ at various H for $\text{Cu}_{0.60}\text{Ta}_2\text{S}_2\text{C}$.

conductivity occurs in these systems. For $\text{Ni}_{0.25}\text{Ta}_2\text{S}_2\text{C}$, with increasing T the difference δ sharply decreases and reduces to a weakly H -dependent positive value above the critical temperature $T_{cu}(H)$. Then $T_{cu}(H)$ can be determined directly from the data of δ vs T . We note that T_{cu} thus obtained is rather different from the local minimum temperature of $d\delta/dT$ as well as the local maximum temperatures of $d\chi_{ZFC}/dT$ vs T and $d\chi_{FC}/dT$ vs T , partly because of the magnetic contribution from Ni^{2+} spins. Figure 13(b) shows the H - T diagram for $\text{Ni}_{0.25}\text{Ta}_2\text{S}_2\text{C}$, where $T_{cu}(H)$ thus obtained is plotted as a function of H . The least-squares fit of the critical line to Eq.(5) yields the parameters, $H_{c2}^{(u)}(0) = 52.0 \pm 11.0$ kOe, $T_{cu} = 8.7 \pm 0.1$ K, and $\alpha(u) = 1.57 \pm 0.12$. For $\text{Cu}_{0.60}\text{Ta}_2\text{S}_2\text{C}$, in contrast, the difference δ gradually decreases with increasing T around T_{cu} , which may be due to a broad distribution of T_{cu} . The critical temperature $T_{cu}(H)$ is defined as a temperature at which the data of $d\delta/dT$ vs T has a local minimum. In Fig. 13(c) we show the H - T diagram for $\text{Cu}_{0.60}\text{Ta}_2\text{S}_2\text{C}$, where $T_{cu}(H)$ is plotted as a function of H . For comparison, we make a plot of the temperature at which the data of $d\chi_{ZFC}/dT$ vs T has a local maximum, as a function of H . The least-squares fit of the critical line to Eq.(5) yields the parameters, $H_{c2}^{(u)}(0) = 15.7 \pm 2.2$ kOe, $T_{cu} = 6.4 \pm 0.1$ K, and $\alpha(u) = 1.15 \pm 0.07$. The value of T_{cu} is lower than that for $\text{Co}_{0.33}\text{Ta}_2\text{S}_2\text{C}$ and $\text{Ni}_{0.25}\text{Ta}_2\text{S}_2\text{C}$.

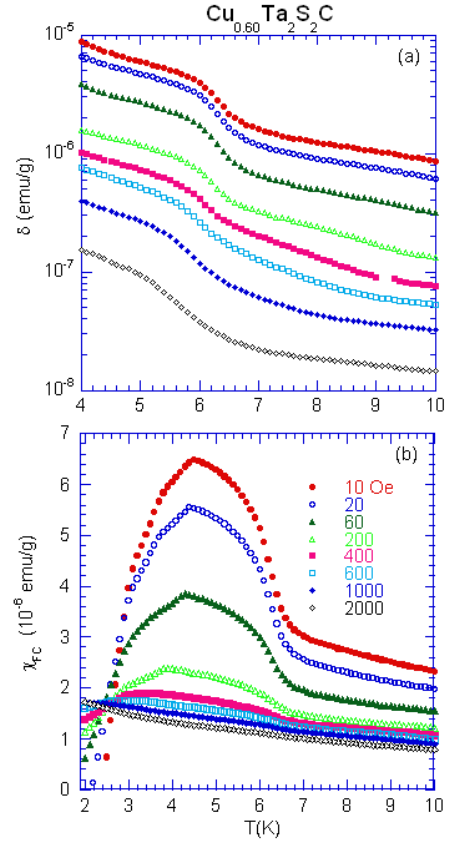


FIG. 17: (Color online) T dependence of (a) δ and (b) χ_{FC} at various H for $\text{Cu}_{0.60}\text{Ta}_2\text{S}_2\text{C}$.

TABLE III: Superconducting parameters of $M_c\text{Ta}_2\text{S}_2\text{C}$ and host $\text{Ta}_2\text{S}_2\text{C}$. There are two transitions at T_{cl} and T_{cu} for $M_c\text{Ta}_2\text{S}_2\text{C}$ and host $\text{Ta}_2\text{S}_2\text{C}$.

$M_c\text{Ta}_2\text{S}_2$	T_c (K)	$H_{c2}(0)$ (kOe)	α
$\text{Fe}^{(u)}$	8.8 ± 0.1	8.3 ± 2.2	1.28 ± 0.14
$\text{Co}^{(u)}$	9.1 ± 0.1	17.1 ± 1.0	1.35 ± 0.06
$\text{Ni}^{(u)}$	8.7 ± 0.1	52.0 ± 11.0	1.57 ± 0.12
$\text{Cu}^{(u)}$	6.4 ± 0.1	15.7 ± 2.2	1.15 ± 0.07
$\text{Fe}^{(l)}, \text{Ni}^{(l)}, \text{Cu}^{(l)}$	4.6 ± 0.1	2.2 ± 0.3	1.25 ± 0.16
$\text{Ta}_2\text{S}_2\text{C}^{(l)}$	3.61 ± 0.01	7.7 ± 0.2	
$\text{Ta}_2\text{S}_2\text{C}^{(u)}$	8.9 ± 0.1	14.0 ± 0.5	1.23 ± 0.07

The critical temperatures T_{cu} in $M_c\text{Ta}_2\text{S}_2\text{C}$ are listed in Table III. If T_{cu} at $c = 0$ ($\text{Ta}_2\text{S}_2\text{C}$) corresponds to T_{cu} ($= 8.9 \pm 0.1$ K), then the lowering of T_{cu} is clearly observed for $\text{Ni}_{0.25}\text{Ta}_2\text{S}_2\text{C}$ and $\text{Cu}_{0.60}\text{Ta}_2\text{S}_2\text{C}$. Similar behavior has been reported by Sakamaki et al.⁷ in $\text{Cu}_c\text{Nb}_2\text{S}_2\text{C}$: $T_c = 7.6$ K at $c = 0$ and $T_c = 4.8$ K for $c = 0.70$. In $M_cX_2\text{S}_2\text{C}$ ($X = \text{Nb}, \text{Ta}$), there is an electron charge transfer from the M_c atoms to the host lattice $X_2\text{S}_2\text{C}$. The increase of conduction electrons leads to the lowering of T_c .

In Fig. 17, χ_{FC} shows a broad peak (or a cusp) near the temperature T_{cl} ($= 4.6$ K) for $\text{Cu}_{0.60}\text{Ta}_2\text{S}_2\text{C}$. This peak shifts to the low- T side with increasing H . Similar behaviors are observed in the form of either a cusp or a kink at $T_{cl}(H)$ in both χ_{FC} and χ_{ZFC} for $\text{Ni}_{0.25}\text{Ta}_2\text{S}_2\text{C}$ and $\text{Fe}_{0.33}\text{Ta}_2\text{S}_2\text{C}$. These data of $T_{cl}(H)$ vs H for $\text{Ni}_{0.25}\text{Ta}_2\text{S}_2\text{C}$ and $\text{Cu}_{0.60}\text{Ta}_2\text{S}_2\text{C}$ are shown in Fig. 9(a). The critical line $H_{c2}^{(l)}(T)$ is described by a power law form similar to Eq.(5) with $T_{cl} = 4.6 \pm 0.1$ K, $H_{c2}^{(l)}(0) = 2.2 \pm 0.3$ kOe, and $\alpha(l) = 1.25 \pm 0.16$. We find that all the data of T_{cl} vs H fall on the critical line $H_{c2}^{(l)}(T)$ common to our all systems.

The effective magnetic moment P_{eff} of $\text{Ni}_{0.25}\text{Ta}_2\text{S}_2\text{C}$ and $\text{Cu}_{0.60}\text{Ta}_2\text{S}_2\text{C}$ is much smaller than the spin-only values. In fact, the g -factors of $\text{Ni}_{0.25}\text{Ta}_2\text{S}_2\text{C}$ ($g = 1.64 \pm 0.02$) and $\text{Cu}_{0.60}\text{Ta}_2\text{S}_2\text{C}$ ($g = 0.324 \pm 0.003$) are much smaller than that observed in Ni^{2+} spin in stage-2 NiCl_2 graphite intercalation compound (GIC) ($g_a = 2.156 \pm 0.002$ and $g_c = 2.096 \pm 0.002$),²⁵ and Cu^{2+} spin in stage-2 CuCl_2 GIC ($g_a = 2.08 \pm 0.01$ and $g_c = 2.30 \pm 0.01$).²⁶ These results suggest that the M ($=$ Ni and Cu) 3d moments are partially delocalized, metallic type of bonding: M 3d electrons are more itinerant. The M 3d states hybridize strongly with the Ta $5d_z^2$ which from the conduction bands of the host compound.

V. DISCUSSION

A. XY symmetry of Fe^{2+} spins

Here we discuss the symmetry of spin Hamiltonian for $\text{Fe}_{0.33}\text{Ta}_2\text{S}_2\text{C}$ with $T_N = 8.7$ K, where the intraplanar exchange interaction is antiferromagnetic. For simplicity, we assume that the parameters of Fe^{2+} spins for $\text{Fe}_{0.33}\text{Ta}_2\text{S}_2\text{C}$ is the same as that of FeCl_2 ; $x = \delta_0/\lambda' = -1.27$, $p = 1.67$, $q = 1.41$, $(p/q)^2 - 1 = 0.40$, $g_c^{(0)} = 3.972$, $g_a^{(0)} = 3.195$, $k = 0.95$, $\lambda' = -67$ cm^{-1} , and $D = 7.0$ $\text{cm}^{-1} = 10$ K (See Sec. II). In the present work, we have measured the average value of g for the powdered sample, which is described by either $g_{av1} = (g_c + 2g_a)/3$ or $g_{av2} = [(g_c^2 + 2g_a^2)/3]^{1/2}$, depending on the form of g :²⁷ $g_{av1} = \langle \cos^2(\theta) \rangle g_c + \langle \sin^2(\theta) \rangle g_a$ or $g_{av2}^2 = \langle \cos^2(\theta) \rangle g_c^2 + \langle \sin^2(\theta) \rangle g_a^2$, where θ is the angle between the magnetic field direction and the z axis, and $\langle \cos^2(\theta) \rangle = 1/3$ and $\langle \sin^2(\theta) \rangle = 2/3$. If $g_a = g_a^{(0)} + \Delta g = 2.91$ and $g_c = g_c^{(0)} = 3.68$ where $\Delta g = -0.29$ is appropriately chosen, then the g -value can be estimated as either $g_{av1} = 3.17$ or $g_{av2} = 3.19$, which are the same as our experimental value $g = 3.16 \pm 0.02$ for $\text{Fe}_{0.33}\text{Ta}_2\text{S}_2\text{C}$. The spin anisotropy parameter D_{eff} can be estimated as $D_{eff} = D(s - 1/2) + (3\Theta/(s + 1))(p^2 - q^2)/q^2 \approx 5 + (-29.5/2)0.4 = -0.9$ K with $s = 1$. The negative sign of D_{eff} suggests the easy-plane type (XY) spin anisotropy of the system: the spins tend to lie in the c plane (perpendicular to the c axis). Thus the Fe^{2+} spins magnetically behave like an XY -like AF on the triangu-

lar lattice.

Here it is interesting to point out that the magnetic properties of $\text{Fe}_{0.33}\text{Ta}_2\text{S}_2\text{C}$ are similar to those of $2H\text{-Fe}_c\text{NbSe}_2$ which belongs to the same universality class: XY -like AF on the triangular lattice. The magnetic properties of $2H\text{-Fe}_c\text{NbSe}_2$ have been extensively studied by Hillenius and Coleman.²⁸ Their results are summarized as follows. The Curie-Weiss temperature Θ of $2H\text{-Fe}_c\text{NbSe}_2$ is negative for $0.05 \leq c \leq 0.33$. At $c = 0.12$ the susceptibility χ_a shows a sharp peak at 12 K with the maximum of 0.092 emu/Fe mole. The susceptibility χ_a is larger than χ_c , suggesting XY anisotropy: $g_a = 2.40$ and $g_c = 2.62$. At $c = 0.33$ the susceptibility χ_a shows a sharp peak at 135 K, suggesting the existence of AF long range order. The maximum susceptibility is 0.02 emu/Fe mole.

In $\text{Fe}_{0.33}\text{Ta}_2\text{S}_2\text{C}$ the interplanar interaction J' is considered to be ferromagnetic but is extremely weak compared with the AF intraplanar exchange interaction. For the 2D XY spin system, a stable spin structure is realized as a 120° spin structure ($\sqrt{3} \times \sqrt{3}$)R 30° commensurate spin structure), where spins rotate successively by 120° . Sakakibara¹⁹ has pointed out that the 120° spin structure becomes unstable by an infinitesimal interplanar exchange interaction J' , and that the incommensurate magnetic structures appear.

B. Ising symmetry of Co^{2+} spins

Next we discuss the spin symmetry of Co^{2+} spin in $\text{Co}_{0.33}\text{Ta}_2\text{S}_2\text{C}$, where the intraplanar exchange interaction is antiferromagnetic. For simplicity, we assume that the parameters of Co^{2+} spins for $\text{Co}_{0.33}\text{Ta}_2\text{S}_2\text{C}$ is the same as that of CoCl_2 : $x = \delta_0/\lambda' = 1.68$, $p = 1.36$, $q = 1.81$, $(p/q)^2 - 1 = -0.44$, $g_c^{(0)} = 3.23$, $g_a^{(0)} = 4.69$, and $k = 0.90$. If $g_a = g_a^{(0)} + \Delta g = 3.15$ and $g_c = g_c^{(0)} + \Delta g = 4.61$ where $\Delta g = -0.08$ is appropriately chosen, then the g -value can be estimated as either $g_{av1} = 4.12$ or $g_{av2} = 4.18$, which are the same as our experimental value $g = 4.12 \pm 0.05$ for $\text{Co}_{0.33}\text{Ta}_2\text{S}_2\text{C}$. For $\text{Co}_{0.33}\text{Ta}_2\text{S}_2\text{C}$, the spin anisotropy parameter can be estimated as $2zsJ_A = (3\Theta/(s + 1))(p^2 - q^2)/q^2 \approx 23.1$ K with $s = 1/2$ and $\Theta = -26.3$ K. The positive sign of J_A suggests the Ising spin anisotropy of the system: the spins tend to align along the c axis. The AF phase transition occurs at $T_N (= 18.6$ K). Note that T_N is lower than $|\Theta| (= 26.3$ K), because of the deviation of molecular field theory. The ratio $\eta (= T_N/|\Theta|)$ is equal to 0.70, which is close to $\eta (= 0.65)$ for CoCl_2 .^{21,22} The Co^{2+} spins magnetically behave like an Ising-like AF on the triangular lattice. A spin frustration effect arising from a macroscopic number of degenerate ground states suppresses the growth of the long range spin ordering. CsCoCl_3 ,²⁹ which is one of the best known systems, undergoes two phase transitions at $T_{N1} (= 21$ K) and $T_{N2} (= 9$ K). In the intermediate phase between T_{N1} and

T_{N2} , spins on two of the three sublattices order antiferromagnetically and the rest remains paramagnetic, forming a so-called partially disordered (PD) phase. Two peaks of both χ_{ZFC} and χ_{FC} in $\text{Co}_{0.33}\text{Ta}_2\text{S}_2\text{C}$ at T_N and T_{cu} may corresponds to T_{N1} and T_{N2} , although T_{cu} is regarded as a superconducting transition point (see Sec. IV D). We note that similar behavior is also observed in $(\text{CeS})_{1.16}[\text{Fe}_{0.33}(\text{NbS}_2)_2]$,³⁰ which is also a quasi 2D Ising AF on the triangular lattice. This system undergoes phase transitions at T_{N1} ($= 22$ K) and T_{N2} ($= 15$ K). The intermediate phase between T_{N1} and T_{N2} is a PD phase.

C. Nature of superconductivity

What is the nature of the superconducting transition at T_{cl} ($= 4.6$ K)? Both χ_{ZFC} and χ' show an anomaly at T_{cl} , which is independent of the kind of M in $M_c\text{Ta}_2\text{S}_2\text{C}$. The critical line $T_{cl}(H)$ is almost the same for $M = \text{Fe}$, Ni , and Cu . The value of T_{cl} is slightly larger than that of T_{cl} for the host $\text{Ta}_2\text{S}_2\text{C}$, partly because of a suppression of the possible CDW. This superconductivity at T_{cl} can coexist with the AF long range spin order below T_N in $\text{Fe}_{0.33}\text{Ta}_2\text{S}_2\text{C}$ and $\text{Co}_{0.33}\text{Ta}_2\text{S}_2\text{C}$. As listed in Table III, the exponent α for $\text{Co}_{0.33}\text{Ta}_2\text{S}_2\text{C}$ and $\text{Ni}_{0.33}\text{Ta}_2\text{S}_2\text{C}$ is on the same order as those for quasi 2D superconductors such as Pd-MG (metal graphite) ($\alpha = 1.43 \pm 0.05$ and $T_c = 3.82 \pm 0.04$ K)³¹ and Sn-MG ($\alpha = 1.43 \pm 0.05$ and $T_c = 3.90 \pm 0.08$ K).³² In these MG's, metal (Pd and Sn) layers, which are sandwiched between adjacent graphene sheets, exhibit superconductivity. Note that the exponent α of $M_c\text{Ta}_2\text{S}_2\text{C}$ is close to that ($= 1.50$) predicted from the de Almeida and Thouless³³ theory for spin glass

behaviors. This result suggests that the critical line may correspond to an irreversibility line where the difference δ starts to increase with decreasing T .

VI. CONCLUSION

$M_c\text{Ta}_2\text{S}_2\text{C}$ exhibits a variety of superconducting and magnetic properties. $\text{Fe}_{0.33}\text{Ta}_2\text{S}_2\text{C}$, which is a quasi 2D XY-like antiferromagnet on the triangular lattice, undergoes an AF transition at T_N ($= 117$ K). The irreversible effect of magnetization occurs below T_N , reflecting the 2D frustrated nature of the system. The AF phase coexists with the superconducting phase below T_{cu} ($= 8.8$ K). $\text{Co}_{0.33}\text{Ta}_2\text{S}_2\text{C}$, which is a quasi 2D Ising antiferromagnet on the triangular lattice, shows an AF transition at $T_N = 18.6$ K. The AF phase coexists with the superconducting phase below $T_{cu} = 9.1$ K. Both $\text{Ni}_{0.25}\text{Ta}_2\text{S}_2\text{C}$ and $\text{Cu}_{0.60}\text{Ta}_2\text{S}_2\text{C}$ are superconductor with $T_{cu} = 8.7$ K and 6.4 K, respectively. $M_c\text{Ta}_2\text{S}_2\text{C}$ also exhibits another superconducting transition at T_{cl} ($= 4.6$ K), which is common to our all systems and is a little higher than that of the host $\text{Ta}_2\text{S}_2\text{C}$ ($T_{cl} = 3.61$ K).

Acknowledgments

The authors are grateful to Pablo Wally, Technical University of Vienna, Austria (now Littlefuse, Yokohama, Japan) for providing us with the samples. One of the authors (J.W.) acknowledges financial support from the Ministry of Cultural Affairs, Education and Sport, Japan, under the grant for young scientists no. 70314375 and from Kansai Invention Center, Kyoto, Japan.

* suzuki@binghamton.edu

† itsuko@binghamton.edu

‡ juergen.walter@chemiemetall.de; CM Chemiemetall GmbH, Niels-Bohr-Str. 5, Bitterfeld, Germany

¹ O. Beckmann, H. Boller, and H. Nowotny, *Monatshefte für Chemie* **101**, 945 (1970).

² P. Wally and M. Ueki, *J. Alloys and Compounds* **268**, 83 (1998).

³ P. Wally and M. Ueki, *Wear* **215**, 98 (1998).

⁴ J. Walter, H. Shioyama, and S. Hara, *J. Vac. Sci. Technol. B* **18**, 1203 (2000).

⁵ J. Walter, W. Boonchuduang, and S. Hara, *J. Alloys and Compounds* **305**, 259 (2000).

⁶ H. Boller and K. Hiebl, *J. Alloys and Compounds* **183**, 438 (1992).

⁷ K. Sakamaki, H. Wada, H. Nozaki, Y. Ōnuki, and M. Kawai, *Solid State Commun.* **118**, 113 (2001).

⁸ J. Walter, I.S. Suzuki, and M. Suzuki, *Phys. Rev. B* **70**, 064519 (2004).

⁹ P. Wally and M. Ueki, *J. Solid State Chem.* **138**, 250 (1998).

¹⁰ H. Boller and R. Sobczak, *Monatshefte für Chemie* **102**,

1226 (1971).

¹¹ J. Kanamori, *Prog. Theor. Phys.* **20**, 890 (1958).

¹² K. Inomata and T. Oguchi, *J. Phys. Soc. Jpn.* **23**, 765 (1967).

¹³ M.E. Lines, *Phys. Rev.* **131**, 546 (1963).

¹⁴ T. Oguchi, *J. Phys. Soc. Jpn.* **20**, 2236 (1965).

¹⁵ F.J. DiSalvo and J.V. Waszczak, *Phys. Rev. B* **22**, 4241 (1980).

¹⁶ H. Boller, private communication (2003).

¹⁷ H. Suematsu, K. Ohmatsu, and R. Yoshizaki, *Solid State Commun.* **38**, 1103 (1981).

¹⁸ M. Date, T. Sakakibara, K. Sugiyama, and H. Suematsu, *High Field Magnetism*, edited by M. Date (North-Holland Publishing Company, 1983) p.41.

¹⁹ T. Sakakibara, *J. Phys. Soc. Jpn.* **53**, 3607 (1984).

²⁰ R.J. Birgeneau, W.B. Yelon, E. Cohen, and J. Makovsky, *Phys. Rev. B* **5**, 2607 (1972).

²¹ C. Starr, F. Bitter, and A.R. Kaufmann, *Phys. Rev.* **58**, 977 (1940).

²² M.T. Hutchings, *J. Phys. C: Solid State Phys.* **6**, 3143 (1973).

²³ P.A. Lindgård, R.J. Birgeneau, J. Als-Nielsen, and H.J.

- Guggenheim, J. Phys. C: Solid State Phys. **8**, 1059 (1975).
- ²⁴ See for example, J.B. Ketterson and S.N. Song, *Superconductivity* (Cambridge University Press, Cambridge, 1999).
- ²⁵ M. Suzuki, K. Koga, and Y. Jinzaki, J. Phys. Soc. Jpn. **53**, 2745 (1984).
- ²⁶ M. Suzuki, I.S. Suzuki, C.R. Burr, D.G. Wiesler, N. Rosov, and K. Koga, Phys. Rev. B **50**, 9188 (1994).
- ²⁷ A. Abragam and B. Bleaney, *Electron Paramagnetic Resonance of Transition Ions* (Oxford University Press, 1970).
- ²⁸ S. J. Hillenius and R.V. Coleman, Phys. Rev. B **20**, 4569 (1979).
- ²⁹ M. Mekata, J. Phys. Soc. Jpn. **42**, 76 (1977).
- ³⁰ C. Michioka, K. Suzuki, and K. Mibu, J. Phys. Soc. Jpn. **71**, 2376 (2002).
- ³¹ M. Suzuki, I.S. Suzuki, and J. Walter, J. Phys. Condensed Matter **16**, 903 (2004).
- ³² M. Suzuki, I.S. Suzuki, and J. Walter, Physica C **402**, 243 (2004).
- ³³ J.R.L. de Almeida and D.J. Thouless, J. Phys. A **11**, 983 (1978).